3D QSAR analysis of oxazolidinone antibacterials: can we predict?

Neha Gandhi*

School of Biomedical Sciences, Curtin University of Technology, Kent Street, Bentley 6845, Western Australia
E-mail: nehagandhioct@rediffmail.com

Abstract
Three-dimensional QSAR studies for substituted aryloxazolidinones **3**–**9** were conducted using TSAR 3.3. The *in vitro* activities (MICs) of the compounds against *Staphylococcus aureus* and *Enterococcus faecalis* exhibited a good correlation with the prediction made by the model using heat of formation and LUMO energies.

Keywords: 3D QSAR, heat of formation, LUMO, antibacterial agent, aryloxazolidinone

Introduction

Multidrug resistant Gram-positive bacteria continue to pose challenges to the medicinal chemistry community.[1] Linezolid **1**, marketed as Zyvox®, is an oxazolidinone class of antibacterial, approved for treating mostly Gram-positive bacterial infections, especially methicillin-resistant *Staphylococcus aureus* (MRSA), *Staphylococcus Epidermidis* (MRSE) and vancomycin resistant enterococci (VRE).[2] Another early clinical candidate, Eperezolid **2**, was discontinued from development after phase I clinical trials. While much research has been aimed at the development of novel oxazolidinones, no new members of this class have achieved regulatory approval.

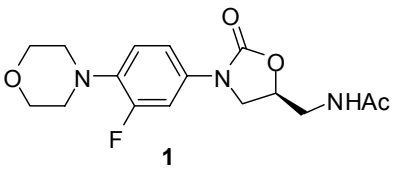

1

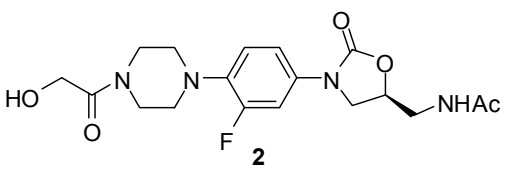

2

In the past, some efforts have been made to understand the structure-activity relationships of oxazolidinone antibacterial agents using comparative molecular field analysis (CoMFA), 3D-QSAR and QSPR methods.[3] We have already reported 3D-QSAR studies for *N*-4-

arylacryloylpiperazin-1-yl-phenyl-oxazolidinones **3–7** using TSAR 3.3.[4] The *in vitro* antibacterial activities (MICs) of compounds **3–7** against *Staphylococcus aureus* ATCC 25923 exhibited a strong correlation with the prediction made by our model. It was observed that the activity of the compounds increases when the energy of the LUMO (Lowest Unoccupied Molecular Orbital) is lower and the heat of formation (HOF) is higher. Thus, compounds which have lower HOF become less active and, similarly, compounds having low LUMO energies are the most active and the activity decreases as the LUMO energy increases.

We decided to examine if our model (Equation 1)[4] can predict the antibacterial activity trends of different sets of compounds **8–9** for the same strain (*S. aureus* ATCC 25923) as well as in a different strain such as *Enterococcus faecalis* (*E. fa*) ATCC 29212.

$$\text{Log (1/C)} = 0.006919662*\text{HOF} - 0.72196823*\text{LUMO} - 0.034151886*\text{Polarization YY} + 0.0004945533*\text{Octupole XYZ} + 4.8290181 \quad (1)$$

The present study aims to validate if compounds **8–9** follow the same parameters for the prediction of their activity, namely, that lower HOF and lower LUMO energies result in more potent antibacterial compounds.

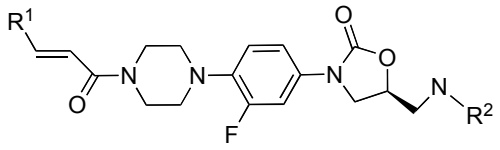

3–**5**

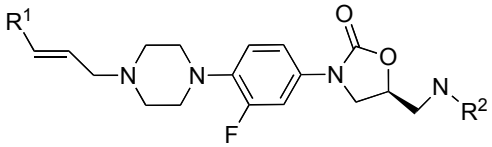

6–**7**

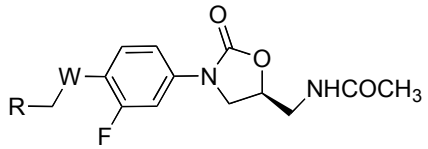

8

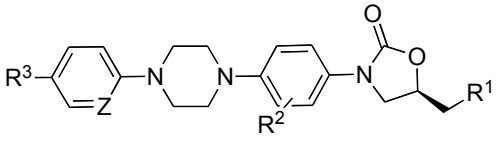

9

Results and Discussion

Based on Equation 1, developed using the training set of compounds reported earlier by us,[4] calculations were done for a set of parameters for compounds **8a** to **8aa**, which is shown in Table 1. A reasonable correlation between the predicted MICs by Equation 1 and the experimental MICs reported by Das *et al.*[5] was observed.

The predicted MICs, especially for **8h**, **8i**, **8j**, **8m**, **8n**, **8q**, **8r** and **8u,** were found to be 8- to 16-fold different from the experimental values. In view of the fact that, generally, reported MICs may vary from laboratory to laboratory by a factor of one dilution (i.e. 2 to 4 or 4 to 8), but some of the above compounds (**8h**, **8i**, **8j**, **8m** and **8r)** needed special deliberation.

Therefore, a new equation (Equation 2) was developed using randomly selected compounds from the training set shown in Table 1 and then used to predict the MIC values for the test

compounds **8b**, **8h**, **8i**, **8j**, **8m**, **8n**, **8q**, **8r** and **8u**. However, the data sets are not suited for QSAR analysis because compounds **8** have very small variance in the biological activities. Nonetheless we wanted to validate the hypothesis that the antibacterial activities follow a trend based on HOF and LUMO energies. The new 3D QSAR model that was obtained is:

$$\text{Log } (1/C) = 0.0068*X1 - 0.7457*X2 + 2.5496 \quad (2)$$

where X1 is Heat of Formation and X2 is LUMO and the statistical parameters for above Equation 2 are: s value = 0.2614; F = 18.3399; regression coefficient r = 0.8507; r^2 = 0.7237; cross validation, r^2(CV) = 0.6045.

With the help of Equation 2, we predicted MIC values for all the compounds (shown in Table 1). Surprisingly, it was found that the predicted MIC values based on both Equations 1 and 2 were significantly different from the experimental values for the same set of compounds (**8h**, **8i**, **8j**, **8m**, **8n**, **8q**, **8r** and **8u**). Thus, a re-examination of the SAR of these compounds was done and it was found that both Equations 1 and 2 are not capable of predicting the difference between the positional isomers. For example, when we compare **8g**, **8q** and **8r**, the predicted MICs remain more or less the same (**8g**, 1.33; **8q**, 1.06; **8r**, 0.6 μg/mL), whereas observed MIC values vary significantly (**8g**, 1; **8q**, 8; **8r**, 8 μg/mL). Furthermore, the equation appears to be inadequate, especially for compounds having powerful electron withdrawing groups such as CN (**8h**: observed MIC of 16 vs. 0.8 μg/mL predicted with Equation 1 or 2.24 μg/mL predicted with Equation 2) or NO_2 (**8n**: observed MIC of 16 v/s 1.48 μg/mL predicted with Equation 1 or 2.10 μg/mL predicted with Equation 2) (see Table 1).

We also considered that it would be interesting to study if Equation 1 can predict the activity of compounds with a different structural scaffold. Therefore, a study of compounds **9a** to **9ac**, as reported by Jang *et al.*[6] (Table 2), was undertaken. A very good correlation between the predicted MIC using Equation 1 and the observed MIC (compound **9d** to **9ac**) was found, except for compounds **9a–9c** (observed MIC >64 μg/mL versus predicted MIC 2–3 μg/mL). Another equation was developed using 23 compounds listed in Table 2 as training set in order to predict the MIC of the remaining test compounds **9m**, **9o**, **9s**, **9v**, **9ab** and **9ac**. However, the data sets are not suited for QSAR analysis because they have significantly different R_1 residues and 15 compounds have very small variance in the biological activities. However, we wanted to investigate if compounds with a different scaffold that have antibacterial activities follow a trend based on HOF and LUMO energies.

The 3D QSAR model developed is as follows:

$$\text{Log } (1/C) = 0.0070*X1 - 3.1117*X2 - 0.1317*X3 + 9.3684 \quad (3)$$

where X1 is Heat of Formation, X2 is LUMO and X3 is Polarization YY and the statistical parameters for above Equation 3 are: s value = 0.4182; F = 34.5641; regression coefficient r = 0.9193; r^2 = 0.8451; cross validation, r^2(CV) = 0.7246.

Table 1. Prediction of antibacterial activity of piperazinylphenyloxazolidinone[5]

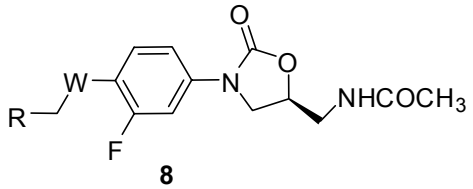

8

Compd.	W	R	Heat of formation	LUMO	Polarization YY	Octupole XXZ	Octupole ZZZ	*S. aureus* ATCC 25923			*E. faecalis* ATCC 29212		
								Experimental MIC (μg/mL)[a]	Predicted MIC (μg/mL)[a] using Equation 1[3]	Predicted MIC (μg/mL)[a] using Equation 2	Experimental MIC (μg/mL)[a]	Predicted MIC (μg/mL)[a] using Equation 4	
8a	piperazine	5-furan	–138.857	–0.483	57.547	51.640	–23.679	8	2.33	4.52	8	11.481	
8b	piperazine	5-furan-2-carbaldehyde	–171.408	–0.523	59.461	–41.400	–16.974	1	3.37	7.45	8	22.545	
8c	piperazine	5-furan-2-carboxylic acid	–226.546	–0.548	60.518	143.518	–36.220	>16	8.44	17.65	>16	14.266	
8d	piperazine	ethyl 5-furan-2-carboxylate	–223.475	–0.536	66.271	162.936	–50.090	>16	15.49	21.07	>16	14.492	
8e	piperazine	5-furan-2-carbaldehyde oxime	–129.767	–0.500	60.600	53.342	–17.558	2	3.25	4.21	8	10.688	
8f	piperazine	(5-furan-2-ylmethylene)-hydrazine	–101.315	–0.541	62.199	–156.048	30.532	2	1.69	2.50	8	18.187	
8g	piperazine	2-nitro-5-furan	–145.305	–1.030	58.786	7.109	–3.658	1	1.33	1.96	2	2.306	
8h	piperazine	5-furan-2-carbonitrile	–100.149	–0.566	61.492	45.497	–11.147	16	0.80	2.24	16	6.386	
8i	piperazine	2-bromo-5-furan	–125.693	–0.499	58.659	70.605	–24.257	>16	1.29	4.21	>16	10.425	
8j	piperazine	2-chloro-5-furan	–142.786	–0.498	58.827	60.863	–34.639	>16	2.56	5.06	>16	12.064	
8k	piperazine	5-furan-2-ylmethanol	–182.986	–0.491	61.661	53.422	7.415	>16	5.90	9.77	>16	15.940	
8l	piperazine	5-furan-2-ylmethyl acetate	–225.982	–0.500	65.699	85.765	–19.444	>16	17.08	20.20	>16	22.807	

8m	piperazine	2-methyl-5-furan	–147.575	–0.474	60.600	50.328	–24.345	>16	3.55	5.42	>16	13.368
8n	piperazine	2-nitro-5-thiophene	–107.413	–1.561	61.037	202.343	–153.299	8	0.45	0.48	8	0.152
8o	piperazine	2-nitro-1*H*-pyrrole	–122.936	–0.705	58.010	195.402	–377.869	4	1.11	3.05	4	7.286
8p	piperazine	1-methyl-2-nitro-1*H*-pyrrole	–122.267	–0.664	60.509	240.185	–376.542	4	1.49	3.13	4	6.822
8q	piperazine	2–nitro-4-furan	–146.711	–1.068	56.872	228.770	–308.339	8	1.06	2.04	8	1.691
8r	piperazine	2-nitro-3-furan	–145.417	–1.007	58.153	–55.671	66.159	8	0.60	2.24	4	2.788
8s	1,4-diazepane	2-nitro-5-furan	–146.145	–1.133	60.568	–1.087	–15.551	2	2.17	2.21	2	1.804
8t	2-methyl-piperazine	2-nitro-5-furan	–150.401	–1.117	61.356	–23.419	–403.063	4	1.62	2.39	4	7.543
8u	(2*S*,6*R*)-2,6-dimethyl-piperazine	2-nitro-5-furan	–156.006	–1.152	61.695	–272.272	374.691	16	1.48	2.10	8	2.260
8v	*N*-methylpiperi-din-4-amine	2-nitro-5-furan	–153.601	–1.036	67.825	–37.910	321.593	1	2.91	2.59	0.5	1.169
8w	*N*-(piperidin-4-yl)acetamide	2-nitro-5-furan	–192.507	–1.412	68.340	300.223	–533.654	>16	5.97	5.54	>16	1.192
8x	piperidin-4-amine	2-nitro-5-furan	–154.942	–1.151	64.747	239.549	–70.990	1	2.66	2.03	0.5	0.626
8y	*N*,3-dimethyl-piperidin-4-amine	2-nitro-5-furan	–156.755	–1.073	68.380	93.588	257.501	>16	3.28	2.91	>16	0.671
8z	(1*R*,5*S*,6*S*)-*N*-methyl-3-aza-bicyclo[3.1.0]-hexan-6-amine	2-nitro-5-furan	–121.769	–1.109	64.627	–99.094	–59.585	2	0.60	1.26	2	3.090
8aa	1-((1*R*,5*S*,6*S*)-3-azabicyclo-[3.1.0]hexan-6-yl)-*N*-methyl-methanamine	2-nitro-5-furan	–123.913	–1.020	56.622	–307.942	545.798	2	0.94	1.36	2	1.943

[a] MIC = Minimum Inhibitory Concentration for inhibition of the organism shown in μg/mL.

Table 2. Prediction of antibacterial activity of arylpiperazinyloxazolidinones with diversification of the *N*-substituents[6]

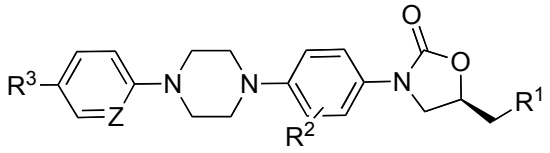

9

Compound	R^1	R^2	R^3	Z	Heat of formation	LUMO	Polarization YY	Octupole XXZ	Octupole ZZZ	*S. aureus* ATCC 25923			*E. faecalis* ATCC 29212	
										Experimental MIC (μg/mL) [a]	Predicted MIC (μg/mL) [a] using Equation 1[3]	Predicted MIC (μg/mL) [a] using Equation 3	Experimental MIC (μg/mL) [a]	Predicted MIC (μg/mL) [a] using Equation 4
9a	2-methoxy-pyridine	F	2-Cl	H	–69.019	–0.419	70.618	68.974	–207.536	>64	3.22	67.46	>64	14.634
9b	2-methoxy-pyrazine	F	2-Cl	H	–100.901	–0.410	67.409	–379.687	–172.397	>64	2.12	22.62	>64	185.924
9c	2-methoxy-isoxazole	F	2-Cl	H	–98.002	–0.501	81.799	41.964	–77.933	>64	3.00	30.92	>64	10.608
9d	$N(C=S)CH_3$	F	H	H	–36.293	–1.055	67.886	320.895	162.382	0.12	0.40	0.15	0.25	0.087
9e	$N(C=S)CH_3$	F	H	N	–31.694	–1.056	65.982	297.511	165.477	0.06	0.36	0.08	0.25	0.093
9f	$N(C=S)CH_3$	F	2-Cl	H	–42.042	–1.053	67.427	307.289	153.329	0.12	0.45	0.14	>64	0.109
9g	$N(C=S)CH_3$	F	3-Cl	H	–42.990	–1.070	66.361	359.197	153.518	0.03	0.46	0.10	0.06	0.079
9h	$N(C=S)CH_3$	F	4-Cl	H	–43.045	–1.074	69.28	361.560	148.908	0.12	0.53	0.28	0.25	0.079
9i	$N(C=S)CH_3$	F	2-Me	H	–44.127	–1.054	64.812	244.794	152.541	0.12	0.23	0.06	0.05	0.147
9j	$N(C=S)CH_3$	F	3-F	H	–79.860	–1.076	73.26	249.192	131.178	0.12	0.80	0.27	0.03	0.198
9k	$N(C=S)SCH_3$	F	H	N	–24.710	–1.306	70.282	148.124	190.185	0.06	0.33	0.04	0.12	0.078
9l	$N(C=S)SCH_3$	F	3-Cl	H	–36.025	–1.326	67.367	193.399	167.930	0.12	0.40	0.04	0.5	0.073
9m	$N(C=S)SCH_3$	H	3-OMe	H	–25.941	–1.238	74.426	183.617	104.352	0.12	0.48	0.16	0.12	0.112
9n	$N(C=S)SCH_3$	F	2-Me	H	–37.149	–1.314	59.888	94.165	152.022	0.12	0.34	0.07	0.12	0.129
9o	$N(C=S)NH_2$	H	H	H	9.138	–0.840	68.874	188.741	289.331	0.12	0.21	0.28	0.12	0.157
9p	$N(C=S)NH_2$	F	H	H	–32.270	–0.902	60.916	262.294	351.767	0.06	0.35	0.06	0.12	0.107
9q	$N(C=S)NH_2$	F	2-OMe	H	–67.144	–0.880	68.165	184.144	347.193	0.25	0.88	0.89	0.25	0.257

9r	$N(C=S)NH_2$	F	H	N	–27.651	–0.899	59.444	253.605	361.004	0.12	0.32	0.05	0.25	0.106
9s	$N(C=S)NH_2$	H	2-Cl	H	3.343	–0.833	69.131	165.825	270.297	0.03	0.26	0.39	0.06	0.220
9t	$N(C=S)NH_2$	F	2-Cl	H	–38.004	–0.891	60.58	267.692	340.235	0.12	0.40	0.05	0.25	0.128
9u	$N(C=S)NH_2$	F	3-Cl	H	–38.968	–0.915	60.009	306.873	368.777	0.02	0.39	0.05	0.06	0.088
9v	$N(C=S)NH_2$	F	3-OMe	H	–70.177	–0.893	65.554	292.509	363.029	0.03	0.93	0.40	0.06	0.137
9w	$N(C=S)NH_2$	F	4-Cl	H	–39.003	–0.907	62.505	252.591	360.425	0.12	0.48	0.10	0.5	0.123
9x	$N(C=S)NH_2$	F	2-Me	H	–40.094	–0.902	64.64	201.658	338.908	0.12	0.52	0.15	0.25	0.169
9y	$N(C=S)NH_2$	F	3-CF_3	H	–190.460	–0.932	53.818	223.300	338.088	0.25	2.59	0.16	0.25	0.584
9z	$N(C=S)OCH_3$	F	H	H	–70.673	–0.822	61.292	265.441	133.243	0.25	0.65	0.21	0.25	0.406
9aa	$N(C=S)OCH_3$	F	H	N	–66.071	–0.813	67.096	238.542	167.998	0.12	1.10	0.97	0.12	0.414
9ab	$N(C=S)OCH_3$	F	3-Cl	H	–77.372	–0.835	65.448	293.138	131.627	0.12	1.30	0.89	0.12	0.385
9ac	$N(C=S)OCH_3$	F	3-OMe	H	–108.607	–0.813	49.076	289.903	133.527	0.12	2.04	3.46	0.12	0.552

[a] MIC = Minimum Inhibitory Concentration for inhibition of the organism shown in μg/mL.

The constant term in Equation 3 is dominant. Therefore, it is instructive to look at the molecular descriptors, based on t value, in the regression model. Descriptors with large $|t|$ values are important in the predictive model and, as such, can be examined in order to gain some understanding of the nature of the property or activity of interest. The descriptors which had higher *t*-values and which appeared with higher frequency in previous models were selected to derive the final regression model. Table 3 indicates the statistical significance of descriptors HOF, LUMO and Polarization YY used in the derivation of Equation 3.

Table 3. Descriptors included in the model

Descriptor	Jacknife SE[a]	Covariance SE[b]	t-value[c]	t-probability[d]
Heat of formation (X1)	0.0076	0.0032	2.4278	0.0247
LUMO (X2)	0.8491	0.5157	–4.583	0.0001
Polarization YY (X3)	0.0245	0.0204	–2.9639	0.0076
Constant (C)	1.5901			

[a] An estimate of the standard error on each regression coefficient derived from a jack-knife procedure on the final regression model.

[b] Gives an estimate of the standard error on each regression coefficient derived from the covariance matrix.

[c] Measures the significance of each variable included in the final model.

[d] Statistical significance for t-values.

The predicted MICs obtained using Equation 3 are shown in Table 2. We found an excellent correlation between the predicted and observed MICs. In all three equations we see a good correlation of activity with HOF and LUMO energies. Therefore, we made plots of C*HOF versus C*LUMO based on Equation 2, where C is a constant coefficient for compounds **8a–8aa** (Figure 1), and for compounds **8a–8ac** based on Equation 3 (Figure 2). It can be observed in these figures that all the compounds that have high HOF and low LUMO energies always have superior antibacterial activities.

Encouraged by these results, a similar equation (Equation 4) for *Enterococcus faecalis* (*E. fa*) ATCC 29212 was developed using randomly selected analogues of compounds **8** and **9** in the training set. Compounds **8c**, **8f, 8h**, **8l**, **8z**, **9e**, **9h**, **9k**, **9r** and **9x** made up the test set. Compounds **8n**, **8w**, **8y**, **9f** were treated as outliers. Equation 4 is:

$$\text{Log } (1/C) = 0.0038735112*X1 - 1.5339189*X2 + 0.0022498923*X3 + 0.001369058*X4 + 1.272866, \quad (4)$$

where X1 is Heat of Formation; X2 is LUMO; X3 is Octupole XXZ and X4 is Octupole ZZZ Component and the statistical parameters for above Equation 4 are: n= 37; s value = 0.36; F = 65.16; regression coefficient r = 0.93; r^2 = 0.88; cross validation, r^2(CV) = 0.83.

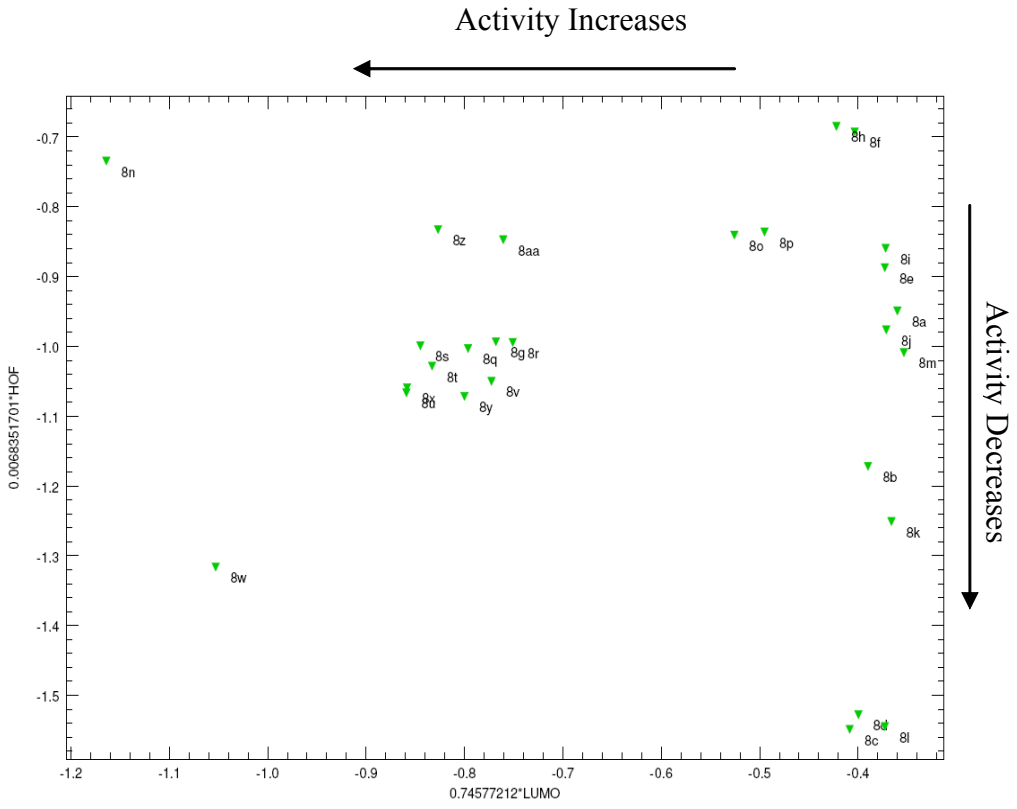

Figure 1. Plot of C*HOF vs. C*LUMO of various training and test set of compounds **8**.

Once again, a very good correlation between the predicted log (1/C) using Equation 4 and the observed log (1/C) was observed for compounds **8** as well as **9** against *E. fa* ATCC 29212. The results are summarised in Tables 1 and 2. The correlation between the observed and the predicted antibacterial activities for the training set and the test set for compounds **8** and **9** using Equation 4 is shown in Figure 3.

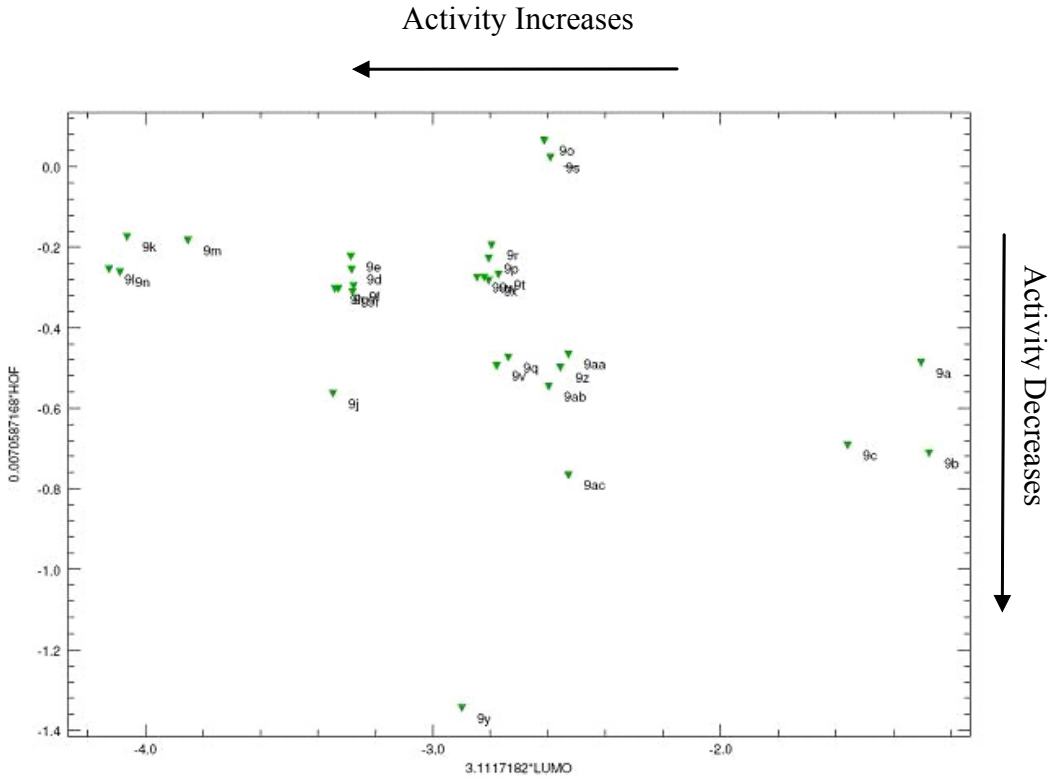

Figure 2. Plot of C*HOF vs. C*LUMO of various training and test set of compounds **9**.

It was expected that such a good correlation between observed and predicted antibacterial activities will also exhibit a close correlation with HOF and LUMO energies. An analysis of the plots of C*HOF vs C*LUMO (figure and values calculated for C*HOF and C*LUMO from Equation 4 are not shown in Tables 1 and 2), where C is a constant coefficient, for compound **8** and compound **9** for *E. fa* ATCC 29212, clearly suggests that for both sets of compounds as the C*HOF increases and C*LUMO decreases, the antibacterial potency of compounds improves and lower MIC values are observed.

It would be worthwhile to examine the antibacterial activities of compounds **3**–**7** in *E. fa* ATCC 29212 and verify if the values predicted (see Table 4) with Equation 4 are comparable to the observed MICs. However, to date there is no antibacterial activity data reported for compounds **3**–**7** for *E. fa* ATCC 29212.

Table 4. Prediction of antibacterial activity of *N*-4-arylacryloylpiperazin-1-yl-phenyl-oxazolidinones[4]

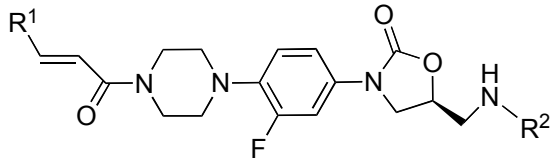

3–**5**

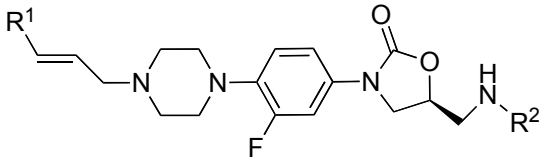

6–**7**

Compound	R^1	R^2	Heat of formation	LUMO	Oct. XXZ	Oct. ZZZ	Predicted log (1/C)[a] for *E. fa* ATCC 29212 using Equation 4.
3a	Ph	COMe	–133.431	–0.836	–79.777	101.405	1.998
3b	4-PhOH	COMe	–178.186	–0.793	59.534	5.055	1.940
3c	3-PhOH	COMe	–178.257	–0.876	–101.717	294.099	2.100
3d	2-thiophene	COMe	–122.886	–1.213	–53.763	211.167	2.825
3e	3-thiophene	COMe	–125.282	–1.000	–51.425	30.985	2.248
3f	2-furan	COMe	–159.744	–0.858	–0.136	260.705	2.326
3g	3-furan	COMe	–161.318	–0.649	32.383	–15.588	1.696
3h	2-1*H*-pyrrole	COMe	–130.927	–0.625	72.798	35.687	1.936
3i	4-pyridine	COMe	–125.392	–1.157	–3.427	–125.293	2.382
3j	3-pyridine	COMe	–125.499	–1.077	–225.370	37.073	1.983
3k	3-1*H*-indole	COMe	–115.993	–0.623	–11.584	226.867	2.064
3l	2-methyl–5-furan	COMe	–168.641	–0.827	–68.720	168.542	1.964
3m	5-furan-2-carbaldehyde	COMe	–191.133	–1.244	–344.990	244.203	1.999
3n	5-furan-2-ylmethanol	COMe	–204.073	–0.831	18.715	204.752	2.079
3o	5-furan-2-ylmethyl acetate	COMe	–246.568	–0.966	–396.949	114.470	1.064
3p	5-furan-2-carboxylic acid	COMe	–246.615	–1.335	–60.717	–419.115	1.654
3q	2-nitro-5-furan	COMe	–164.122	–1.800	320.183	–818.085	2.998
3r	2-nitro-5-thiophene	COMe	–127.101	–2.178	257.376	–1274.840	2.954
3s	1,2-difluorobenzene	COMe	–219.127	–1.257	–53.420	–232.088	1.914
3t	(methylsulfonylmethyl) Ph	COMe	–246.637	–0.973	9.587	295.576	2.236
3u	pyrocatechol	COMe	–221.837	–0.857	34.598	145.605	2.005
3v	*p*-phenyl pivalate	COMe	–227.925	–0.918	–171.486	838.009	2.559
4a	Ph	CSMe	–62.701	–1.032	239.601	470.589	3.796
4b	4-PhOH	CSMe	–108.102	–1.030	434.518	323.365	3.854

4d	2-thiophene	CSMe	–52.838	–1.185	–266.866	105.475	2.430
4f	2-furan	CSMe	–88.649	–1.063	–235.789	126.774	2.203
4i	4-pyridine	CSMe	–55.413	–1.133	23.571	–39.428	2.796
4k	3-1*H*-indole	CSMe	–45.871	–1.041	279.246	270.114	3.690
4q	5-nitro-2-furan	CSMe	–94.655	–1.804	587.221	–677.719	4.066
5a	Ph	$CSNH_2$	–58.606	–0.864	306.107	280.574	3.444
5b	4-PhOH	$CSNH_2$	–104.003	–0.868	511.264	111.319	3.503
5d	2-thiophene	$CSNH_2$	–48.822	–1.155	–263.670	2.967	2.267
5f	2-furan	$CSNH_2$	–84.638	–0.909	–228.015	21.757	1.856
5i	4-pyridine	$CSNH_2$	–50.552	–1.111	–183.405	–343.462	1.898
5k	3-1*H*-indole	$CSNH_2$	–45.035	–0.906	–110.592	132.528	2.421
5v	*p*-phenyl pivalate	$CSNH_2$	–153.077	–0.884	602.704	365.220	3.892
6	2-furan	COMe	–122.747	–0.510	0.971	193.289	1.847
7	2-nitro-5-furan	COMe	–130.648	–1.380	–308.017	–306.049	1.772

[a] C, concentration expressed in mM/L of the drug molecules required for inhibition of 90% growth of *E. fa* ATCC 29212.

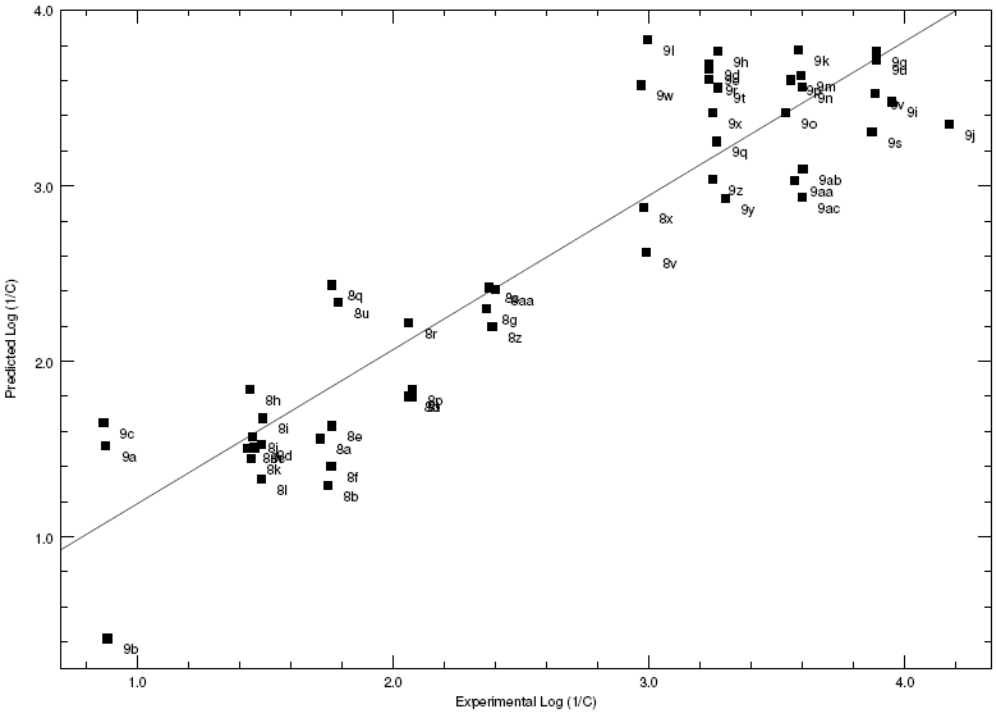

Figure 3. Prediction of antibacterial activity for the training and test set compounds **8**–**9** against *E. fa* ATCC 29212 using Equation 4.

Conclusions

We can conclude that the 3D-QSAR equations based on HOF and LUMO energies enable us to predict the MIC value trends of oxazolidinone antibacterials and in many cases obtain close correlation with experimental MIC values. Calculation of the values of HOF and LUMO energies for compounds containing substitutions can also help to make predictions of antibacterial activities closer to experimental MIC values. For example, phenyloxazolidinones containing substitutions such as CF_3, $COCF_3$, SO_2CH_3, and $SOCHF_2$ have a very low HOF (large negative) and high LUMO energies (high positive). Therefore, we can predict such compounds to show poor antibacterial activity based on predicted log (1/C) values from our 3D-QSAR equations. Substitutions like CN or NO_2 on furan or benzene rings lead to higher HOF (low negative value) and low LUMO energies (large negative) and are thus predicted to show good antibacterial activity for different sets of compounds and in different bacterial strains. These models provide us with a tool to make compounds with predictable antibacterial activities.

Experimental Section

General Procedures. TSAR 3D methods were used to derive 3D-QSAR equations as reported earlier.[4] The structures were sketched using ChemDraw Ultra 5.0 (www.cambridgesoft.com) and were exported to TSAR 3.3 (www.accelrys.com). The three-dimensional structures of all the molecules were generated. Partial charges were derived using the Charge-2 CORINA 3D package in TSAR 3.3 and the geometries of the molecules were optimised using the Cosmic module of TSAR. The calculations were terminated if the energy difference or the energy gradient were smaller than 1e–005 and 1e–010 kcal/mol respectively. The respective MIC values in mg/mL of compounds **8–9** were converted to log (1/C), where C is the concentration expressed in mM/L of the drug molecule required for 90% inhibition of the growth of the microorganism. Data for inactive compounds in the ranges >16 μg/mL, >32 μg/mL and >64 μg/mL are treated as = 16 μg/mL, 32μg/mL and 64μg/mL, respectively, for the training data set and r^2 determination.

Molecular descriptors for the entire molecules were calculated with TSAR 3.3. Vamp, a semiempirical molecular orbital package in TSAR 3.3, was used to calculate electronic properties, including heats of formation, HOMO and LUMO energies, polarizability and multipole components, and to perform structure optimizations in vacuo using default parameters and using the Hamiltonian method PM3. Descriptors with the same values for all compounds **8–9** were discarded. A pair-wise correlation analysis of the remaining descriptors was performed. Regression models were built using descriptor subsets containing only one of these highly correlated descriptors. To develop QSAR models, stepwise MLR analysis with leave-one-out (LOO) cross-validation was applied to the data set. The approach used for the prediction of

antibacterial activities is a simple regression analysis. We refer to these procedures as 3D QSAR methods.

Acknowledgements

I am grateful to Dr. Brijesh Srivastava, Sr. Scientist and Dr. Vidya Lohray, former Vice-President, Zydus Research Centre for their encouragement and continuous support. I also acknowledge Dr. Ricardo Mancera, School of Biomedical Sciences, Curtin University of Technology for his help with the manuscript.

References

1. Service, R. F. *Science* **1995***, 5237,* 724.
2. (a) Swaney, S. M.; Aoki, H.; Ganoza, M. C.; Shinabarger, D. L. *Antimicrob. Agents Chemother.* **1998***, 12,* 3251. (b) Brickner, S. J. *Current Pharmaceutical Design* **1996***, 2,* 175. (c) Zurenko, G. E.; Yagi, B. H.; Schaadt, R. D.; Allison, J. W.; Kilburn, J. O.; Glickman, S. E.; Hutchinson, D. K.; Barbachyn, M. R.; Brickner, S. J. *Antimicrob. Agents Chemother.* **1996***, 4,* 839.
3. (a) Gopalakrishnan, B.; Khandelwal, A.; Rajjak, S. A.; Selvakumar, N.; Das, J.; Trehan, S.; Iqbal, J.; Kumar, M. S. *Bioorg. Med. Chem*. **2003**, 12, 2569. (b) Karki, R. G.; Kulkarni, V. M. *Bioorg. Med. Chem*. **2001**, 12, 3153. (c) Katritzky, A. R.; Fara, D. C.; Karelson, M. *Bioorg. Med. Chem*. **2004**, 11, 3027. (d) Pae, A. N.; Kim, S. Y.; Kim, H. Y.; Joo, H. J.; Cho, Y. S.; Choi, K. I.; Choi, J. H.; Koh, H. Y. *Bioorg. Med. Chem. Lett*. **1999**, 18, 2685. (e) Tokuyama, R.; Takahashi, Y.; Tomita, Y.; Tsubouchi, M.; Yoshida, T.; Iwasaki, N.; Kado, N.; Okezaki, E.; Nagata, O. *Chem. Pharm. Bull*. (Tokyo) **2001**, 4, 353.
4. Lohray, B. B.; Gandhi, N.; Srivastava, B. K.; Lohray, V. B. *Bioorg. Med. Chem. Lett.* **2006***, 14,* 3817.
5. Das, B.; Rudra, S.; Yadav, A.; Ray, A.; Rao, A. V.; Srinivas, A. S.; Soni, A.; Saini, S.; Shukla, S.; Pandya, M.; Bhateja, P.; Malhotra, S.; Mathur, T.; Arora, S. K.; Rattan, A.; Mehta, A. *Bioorg. Med. Chem. Lett.* **2005***, 19,* 4261.
6. Jang, S. Y.; Ha, Y. H.; Ko, S. W.; Lee, W.; Lee, J.; Kim, S.; Kim, Y. W.; Lee, W. K.; Ha, H. J. *Bioorg. Med. Chem. Lett.* **2004***, 15,* 3881.